inter.noise
HAMBURG 2016

Transfer matrices to analyze the acoustic black hole effect in duct terminations

Oriol GUASCH[1]; Marc ARNELA[2]; Patricia SÁNCHEZ-MARTÍN[3]

GTM Grup de recerca en Tecnologies Mèdia, La Salle, Universitat Ramon Llull,

C/ Quatre Camins 2, Barcelona 08022, Catalonia, Spain

ABSTRACT

The acoustic black hole (ABH) effect for sound absorption in duct terminations can be achieved through a combination of two features. First, a power-law decay of the duct radius when approaching the tube end, and second, an appropriate decay of the wall admittance with the duct radius. The latter can be achieved by inserting a set of rigid rings with inner area decreasing to zero at the end of the tube, which constitute the ABH. The corresponding wall admittance can be modeled by means of a lumped compliance per unit surface at the continuum level. Yet in practice, one will have to deal with an imperfect ABH consisting of a finite amount of cavities separated by rings of finite thickness. The performance of such a retarding structure can be analyzed by means of the transfer matrix method for acoustic filters. In this work we do so for an ABH-like tube termination with linear decaying internal radius. The effects of varying the number of cavities, as well as the thickness of the separating rings and damping are investigated.

Keywords: Acoustic black hole, Retarding structure, Waveguide, Transfer matrices, Acoustic filters
I-INCE Classification of Subjects Number(s): 26.1.1, 37.4.

1. INTRODUCTION

The acoustic black hole (ABH) effect is a passive approach to control vibrations and sound. The effect is achieved by means of a retarding structure, or geometry, that induces a power-law decrease of the incident wave velocity with distance. In theory, the wave never reaches the limit of the retarding structure because its speed tends to zero when approaching the boundary. Therefore, no reflection can occur. In practice, one cannot manufacture perfect ABHs and it becomes necessary to place some damping mechanism/material at the area of low velocity to get large vibration or sound reductions. A review on recent advances and applications of ABHs can be found in [1].

To date, most efforts on ABHs have been placed on flexural waves in beams and plates (see e.g. [2,3,4,5,6]). However, much less attention has been paid to the possibility of using ABHs for sound reduction. The first proposal to do so was suggested in [7], where an analysis was made for a retarding structure consisting of rings and cavities placed at the termination of a duct. The wall admittance of that structure was such that when combined with a power-law decaying radius resulted in an ABH effect, with no plane waves reflecting from the end of the duct. Two dimensional designs of ABH sound absorbers were proposed in [8,9], which consisted of a hollow cylindrical porous absorber combined with a graded index metamaterial impedance matching layer.

In this work we will focus on the ABH suggested in [7]. For that retarding structure, both, the wall admittance and the acoustic pressure inside the duct become singular at the duct end section. Consequently, for practical computations of the reflection coefficient one has to assume an imperfect ABH that finishes before the final section of the duct (the situation is somewhat akin to the truncation of potential decaying wedges in plates). However, when building such an ABH that will be not the sole limitation because it will be also necessary to deal with a finite amount of cavities, separated by rings of finite thickness (see [10,11]). The admittance of a real retarding structure will depart from the theoretical one in [7] and thus limit the ABH effect. A detailed analysis of the realistic retarding structure could be performed by means of finite element simulations (FEM). Yet, prior to that it is herein proposed to make use of the transfer matrix method (TMM, see e.g., [12]) for acoustic filters to

[1]oguasch@salle.url.edu
[2]marnela@salle.url.edu
[3]psanchez@salle.url.edu

analyze the influence of various ABH parameters, such as the number of rings/cavities, the impact of the ring thicknesses, the damping, etc. The use of TMM allows one to make fast computations to select a particular ABH design, whose behavior could be then analyzed in more detail using FEM. The case of an ABH with linear decaying radius will be addressed in this paper.

The work is organized as follows. In section 2, we will closely follow [7] and review the theory behind the duct termination ABH proposed therein. In section 3, the TMM theory will be developed to deal with a more realistic exemplification of that ABH retarding structure. Comparisons between the theoretical and realistic ABH behaviors will be presented in section 4, together with the dependence on some design parameters. Conclusions will be finally drawn in section 5.

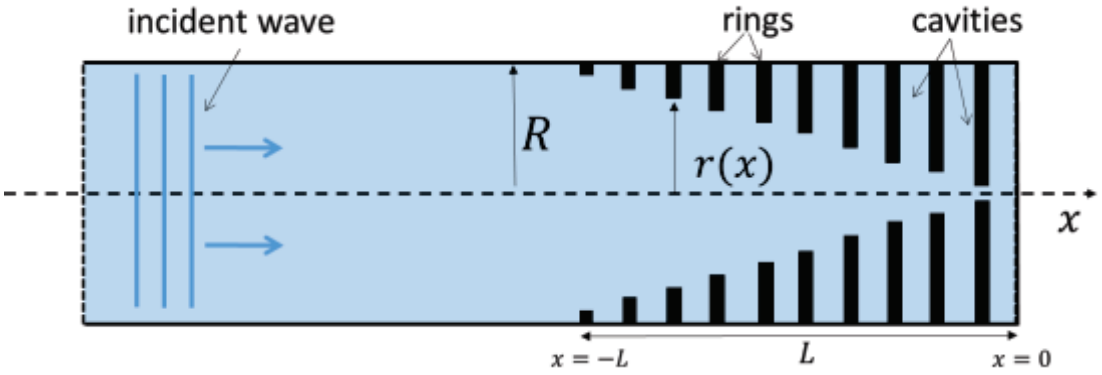

Figure 1 – Retarding structure to produce the ABH effect at the duct termination

2. ACOUSTIC BLACK HOLE EFFECT IN DUCT TERMINATIONS

2.1 Governing equations and solutions for radius linear decay

The equation governing plane wave propagation in an axisymmetric duct of varying cross-section $S(x)$ and wall admittance $Y(x)$ is given by a slight generalization of the Webster equation. In the case of time harmonic dependence in time, $p(x,t) = p(x)\mathrm{e}^{-j\omega t}$, that becomes (see [7]),

$$\partial_{xx}^2 p + \partial_x p \partial_x(\ln S) + p\left[k_0^2 + j\omega\frac{2Y\rho_0}{r}\right] = 0, \tag{1}$$

where x stands for the coordinate on the duct symmetry axis (its origin $x = 0$ being placed at the duct termination) and $r(x)$ denotes the tube radius. ρ_0 represents the air density, $k_0 = \omega/c_0$ the wavenumber and c_0 the speed of sound.

Let us consider a rigid duct of constant radius R and place a retarding structure at its termination end starting at $x = -L$, with the goal that any wave incident on it experiences no reflection (see Figure 1). We need two requisites to achieve that purpose: first, a power-law decay to zero of the retarding structure radius $r(x)$, and second, an appropriate dependence of the wall admittance $Y(x)$ with $r(x)$. As regards the former, in this work we will only consider the case of linear decay, $r = -(R/L)x$. On the other hand, if the structure consists of a set of rigid rings of inner radius $r(x)$, close to each other, and separated by air cavities, the wall admittance can be approximated by a continuous lumped compliance (see [1], and section 3.1)

$$Y = -j\frac{k_0}{Z_0}\frac{R^2 - r^2}{2r}. \tag{2}$$

Note that $Y(x)$ becomes singular at $r = 0$. Substituting (2) in (1) and taking into account the radius linear decay results in

$$\partial_{xx}^2 p + (2/x)\partial_x p + (k_0 L/x)^2 p = 0. \tag{3}$$

This equation admits a general solution of the type

$$p(x) = C_1 \exp[\alpha_1 \ln x] + C_2 \exp[\alpha_2 \ln x], \tag{4}$$

with C_1 and C_2 standing for real constants and

$$\alpha_{1,2} = (1/2)\left[-1 \pm \sqrt{1-(2k_0L)^2}\right]. \tag{5}$$

Therefore, for $k_0L > 0.5$ the solution will exhibit an oscillatory behavior. Note that (4) is nothing but the power-law solution in [7] that has been written in this way for convenience. The imaginary part of the exponent in the first term of (4) can be understood as that corresponding to a wave that propagates to the right with local wavenumber, $k(x)$, such that

$$\int_{-L}^{x} k(x)dx = (1/2)\ln x \sqrt{(2k_0L)^2 - 1}. \tag{6}$$

Consequently we get

$$k(x) = (1/2x)\sqrt{(2k_0L)^2 - 1}. \tag{7}$$

The reason why the ABH effect takes place can now be made apparent. For a wave packet entering the retarding structure at $x = -L$, the group velocity will be

$$c_g = (\partial k/\partial\omega)^{-1} = (c_0^2 x/2L^2\omega)\sqrt{(2k_0L)^2 - 1}, \tag{8}$$

so the time it takes for the wave packet to reach the end of the duct will be given by

$$T = \lim_{l\to 0^-} \int_{-L}^{-l}(1/c_g)dx = \lim_{l\to 0^+} \frac{L^2\omega}{2c_0^2\sqrt{(2k_0L)^2-1}} \ln\left(\frac{L}{l}\right) \to \infty. \tag{9}$$

In other words, a wave entering the retarding structure will never reach its end so no wave will be reflected from it.

2.2 Reflection coefficient from an imperfect ABH

It is clear from (4)-(5) that the acoustic pressure becomes singular at the origin as it does the wall admittance (2). This implies that to characterize the black hole we need to assume that the retarding structure does not extend to the origin, but stops at a finite distance $x = -l$, with $-L < x < -l$. Imposing pressure and velocity continuity at $x = -L$ and a boundary condition at $x = -l$ characterized by an admittance Y_l, it is possible to derive the following expression for the reflection coefficient, R_L, at the entrance of the waveguide (see [7] for the derivation),

$$R_L = \frac{1+R_l+\frac{1}{jk_0L}(\alpha_1+R_l\alpha_2)}{1+R_l-\frac{1}{jk_0L}(\alpha_1-R_l\alpha_2)} e^{-2jk_0L}, \text{ with } R_l = -\frac{\alpha_1+jk_0Z_0lY_l}{\alpha_2+jk_0Z_0lY_l}\left(\frac{l}{L}\right)^{\alpha_1-\alpha_1}. \tag{10}$$

The fact that the retarding structure ends at $x = -l$ constitutes a first imperfection of the ABH. In addition, and as stated earlier in the Introduction, when trying to implement one into practice many more limitations will be found, which are related to the number and size of the cavities taken into account, the thickness of the inner rings, etc. Consequently, the wall admittance of the waveguide can depart from the theoretical value in (2), resulting in a reflection coefficient different from (10). As shown in the next section, the theory of transfer matrices for acoustic filters offers a simple way to analyze the influence of those parameters.

3. TRANSFER MATRICES

3.1 Combined transfer matrix for a cavity plus ring ensemble

To get a closer representation of a realistic retarding structure we will simulate it as an acoustic filter consisting of several cavities connected by short cylindrical ducts delimitated by the thicknesses of the inner radii of the rings (see Figure 2).

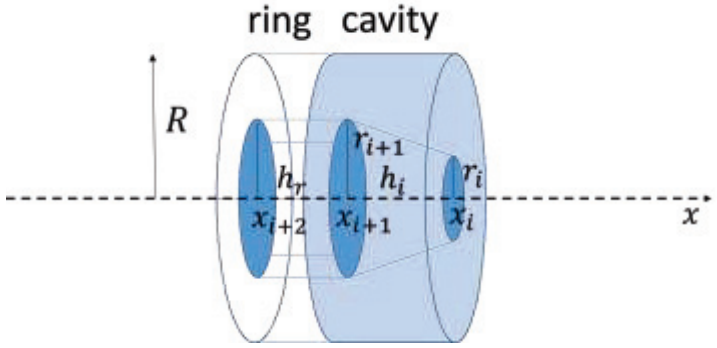

Figure 2 – Solid ring connected to a cavity limited by an inner virtual truncated cone surface and the duct walls.

Let us first focus on the latter. The TMM allows one to relate the acoustic pressure and the acoustic particle velocity at section x_{i+2} to those at x_{i+1} through the propagation matrix $\boldsymbol{T}_{i+1}^{ring}$

$$\begin{pmatrix} p_{i+2} \\ v_{i+2} \end{pmatrix} = \begin{bmatrix} \cos(k_0 h_r) & -jZ_0 \sin(k_0 h_r) \\ -j\sin(k_0 h_r)/Z_0 & \cos(k_0 h_r) \end{bmatrix} \begin{pmatrix} p_{i+1} \\ u_{i+1} \end{pmatrix} \equiv \boldsymbol{T}_{i+1}^{ring} \begin{pmatrix} p_{i+1} \\ v_{i+1} \end{pmatrix}, \tag{11}$$

with $h_r \equiv |x_{i+2} - x_{i+1}|$ standing for the thickness of the ring (held constant for all of them).

On the other hand, the cavities comprise the space between two consecutive rings and have an inner virtual surface that corresponds to a truncated cone. The *i*-th cavity extending from coordinates x_i to x_{i+1} will thus have a volume

$$V_i = \pi h_i \left[R^2 - \frac{1}{3}(r_{i+1}^2 + r_i^2 + r_{i+1} r_i) \right], \tag{12}$$

with $h_i \equiv |x_{i+1} - x_i|$ being the cavity width and r_i standing for the inner radius of the ring at section x_i. The cavity admittance will be given by

$$Y_i^{cav} = -jk_0 V_i / Z_0 \ . \tag{13}$$

Taking into account that the surface of the truncated cone is $S_i = \pi(r_{i+1} + r_i)\sqrt{h_i^2 + (r_{i+1} - r_i)^2}$, it can readily be checked through division of Y_i^{cav} by S_i and by taking the limit $x_{i+1} \to x_i$, that we recover the continuous admittance in (2).

The TMM approach models the influence of a lateral cavity as a lumped element. To take into account the effects of its finite thickness h_i we should combine the lumped matrix with a propagation one. The acoustic pressure and acoustic particle velocity at section x_{i+1} can then be obtained from those at x_i by means of

$$\begin{aligned} \begin{pmatrix} p_{i+1} \\ v_{i+1} \end{pmatrix} &= \begin{bmatrix} \cos(k_0 h_i) & -jZ_0 \sin(k_0 h_i) \\ -j\sin(k_0 h_i)/Z_0 & \cos(k_0 h_i) \end{bmatrix} \begin{bmatrix} 1 & 0 \\ Y_i^{cav}/S_{i+1} & S_i/S_{i+1} \end{bmatrix} \begin{pmatrix} p_i \\ v_i \end{pmatrix} \\ &= \begin{bmatrix} \cos(k_0 h_i) - (k_0 V_i/S_{i+1}) \sin(k_0 h_i) & -j(Z_0 S_i/S_{i+1}) \sin(k_0 h_i) \\ -\frac{j}{Z_0}[\sin(k_0 h_i) + (k_0 V_i/S_{i+1}) \cos(k_0 h_i)] & (S_i/S_{i+1}) \cos(k_0 h_i) \end{bmatrix} \equiv \boldsymbol{T}_i^{cav} \begin{pmatrix} p_i \\ v_i \end{pmatrix}, \end{aligned} \tag{14}$$

where (12) has been taken into account and we have identified the cavity transfer matrix $\boldsymbol{T}_i^{cav}$ in the second equality.

Equations (11) and (14) can be combined to obtain the acoustic pressure and velocity at the entrance x_{i+2} of the combined set ring plus cavity, with those at the exit x_i as

$$\begin{pmatrix} p_{i+2} \\ v_{i+2} \end{pmatrix} = \boldsymbol{T}_{i+1}^{ring} \boldsymbol{T}_i^{cav} \begin{pmatrix} p_i \\ u_i \end{pmatrix}$$

$$= \begin{bmatrix} \cos[k_0(h_r+h_i)] - (k_0 V_i/S_{i+1}) \sin[k_0(h_r+h_i)] & -j(Z_0 S_i/S_{i+1}) \sin[k_0(h_r+h_i)] \\ -\frac{j}{Z_0}\{\sin[k_0(h_r+h_i)] + \left(\frac{k_0 V_i}{S_{i+1}}\right)\cos[k_0(h_r+h_i)]\} & \frac{S_i}{S_{i+1}}\cos[k_0(h_r+h_i)] \end{bmatrix} \quad (15)$$

$$\equiv \boldsymbol{T}_{i+1} \begin{pmatrix} p_i \\ v_i \end{pmatrix}.$$

Damping can be introduced into the system by considering a complex wavenumber in (15).

3.2 Transfer matrix for the retarding structure and reflection coefficient

It is possible to relate the acoustic pressure and acoustic particle velocity between an arbitrary section at x_{k+2} with those at x_i $(k \geq i+2)$ by means of subsequent products of matrices $\boldsymbol{T}_{i+1}$ in (15). Let us define the matrix

$$\boldsymbol{A}(k+2, i) \equiv \prod_{m=i}^{k+1} \boldsymbol{T}_{m+1}, \quad (16)$$

so that

$$\begin{pmatrix} p_{k+2} \\ v_{k+2} \end{pmatrix} = \boldsymbol{A}(k+2, i) \begin{pmatrix} p_i \\ v_i \end{pmatrix}. \quad (17)$$

In particular, if we consider a whole structure with N rings/cavities we get

$$\begin{pmatrix} p_N \\ u_N \end{pmatrix} = \boldsymbol{A}(N, 0) \begin{pmatrix} p_0 \\ u_0 \end{pmatrix}. \quad (18)$$

By the way, note that if the first cavity has rigid walls then $u_0 = 0$.

The admittance at the entrance $x = -L$ of the retarding structure turns to be

$$Y_L = \frac{u_N}{p_N} = \frac{A_{21} p_0 + A_{22} u_0}{A_{11} p_0 + A_{12} u_0} = \frac{A_{21} + A_{22} Y_{l=0}}{A_{11} + A_{12} Y_{l=0}}, \quad (19)$$

$Y_{l=0}$ denoting the admittance at $x = 0$. The reflection coefficient at $x = -L$ will be finally given by

$$R_L^{TM} = \frac{1 + Z_0 Y_L}{1 - Z_0 Y_L}, \quad (20)$$

which is to be compared with the reflection coefficient (10) for the theoretical ABH.

4. NUMERICAL TESTS

4.1 Analytical results

Let us first focus on the results derived from the analytical expressions for the ABH reflection coefficient in (10). To that purpose, we consider a cylindrical duct with length $L = 0.5$ m and radius $R = 0.23$ m. The cutting frequency for this duct is $f_c = 1.84 c_0/R = 2720$ Hz, which leads to a maximum value for the non-dimensional number $k_0 L$ of 4. Let us adopt the value $c_0 = 340$ m/s for all simulations and introduce also damping into the system by means of a complex speed of sound $c = c_0(1 + 0.05j)$, unless specified.

In the particular case of having an anechoic termination at $x = 0$ so that $R_{l=0} = 0$, the reflection coefficient at the entrance of the retarding structure R_L in (10) performs as depicted in Figure 3 (black line). Total reflection occurs whenever $k_0 L < 0.5$ as predicted by (5). However, the reflection coefficient rapidly diminishes for increasing $k_0 L$, as observed, resulting in a notorious ABH effect that

could be even enhanced by increasing the damping (see section 4.3 later). However, if we no longer assume that $R_{l=0} = 0$ and consider a rigid end section (vanishing acoustic particle velocity at the end wall), the reflection coefficient (10) can no longer be computed at $x = 0$. This is so because, as mentioned earlier, both the acoustic pressure and the wall admittance become singular at this point. It becomes then necessary to assume a certain imperfection at the duct and make it terminate at a distance $x = -l$ from the origin. The effects of doing so on R_L are drastic as appreciated in Figure 3 (blue dashed line) even if small values of l are contemplated ($l = 1$ mm has been taken in Figure 3). Peaks and dips appear and the ABH effect clearly deteriorates, though depending on damping still small values could be obtained for the reflection coefficient R_L . This type of behavior was already reported in [7], where the current retarding structure was first proposed and analyzed.

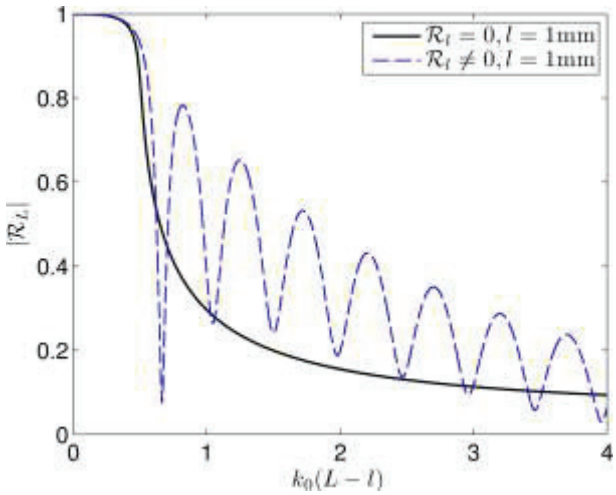

Figure 3 – Reflection coefficient R_L of the retarding structure for the cases of no reflection at the duct termination (black line) and rigid end termination (dashed blue line)

4.2 Influence of the number of cavities

As long as one aims at building a practical realization of the ABH in Figure 1 (see e.g., [10,11]) several considerations come to mind. First, one could wonder how many rings and cavities and of which sizes are necessary to recover the results predicted by the analytical formulation. The transfer matrix approach in section 3 offers a way to address those issues. Let us analyze in this section the effects of the number of cavities on the retarding structure reflection coefficient. It is to be mentioned that only the case of equal spaced rings of constant thickness will be considered in this work, unequal ring distribution being left for forthcoming developments.

In order to separate the effects of the various parameters playing a role, in this subsection we consider the case of very thin rings of thickness $h_r = 1\,\mu$m. The influence of the number of rings/cavities is shown in Figures 4a and b where we plot the reflection coefficient for imperfect ABHs with $l = 10^{-3}$m and $l = 3x10^{-3}$m, respectively. Figure 4 presents the analytical R_L from (10) (black continuous line in the figure) and compares it with that of the transfer matrix method, R_L^{TM} in (20), when varying the total number *N* of rings. As expected, R_L^{TM} tends to the analytical curve R_L when increasing *N*, but the number of rings needed to do so quickly increases. This poses a severe limitation to practical realizations of the ABH, which aim at a limited number of rings for manufacturing purposes.

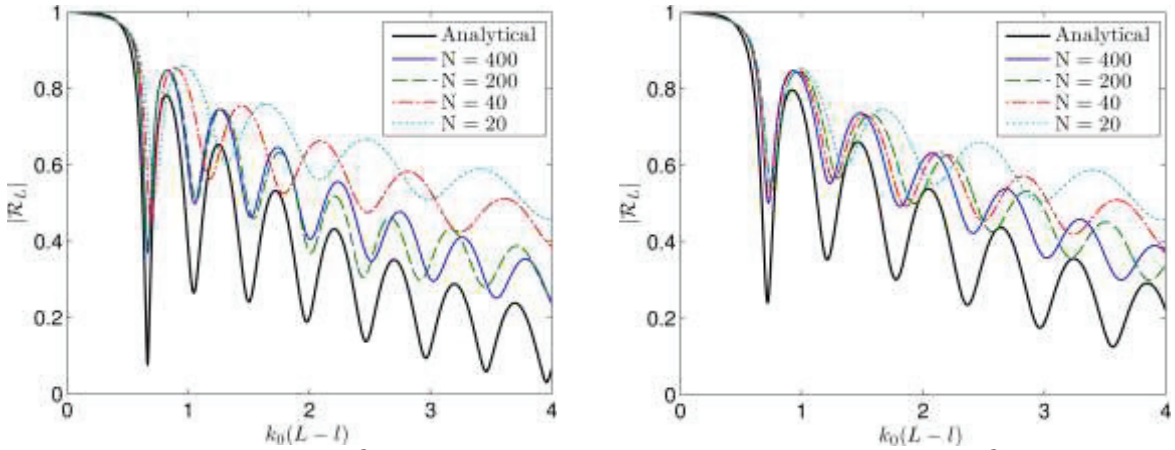

a) $l = 10^{-3}$m b) $l = 3x10^{-3}$m

Figure 4 – Influence of the number of rings/cavities on the retarding structure reflection coefficient for fixed ring thickness and damping.

On the other hand it can be observed by direct comparison of Figures 4a and b that augmenting the value of the imperfection l logically increases the value of the reflection coefficient yet the number of oscillations in it becomes reduced.

4.3 Influence of the ring thicknesses

Let us next analyze the effects of modifying the ring thickness on the reflection coefficient R_L^{TM} of the retarding structure. To proceed we fix the number of cavities to $N = 40$ and change h_r from the very small value of $h_r = 1\,\mu$m to those of $h_r = 1, 2, 4$ mm (2 mm thickness rings were used, for instance, in the retarding structures built in [10,11]). In Figures 5a and b we present the results for the two imperfect ABHs of the previous section with $l = 10^{-3}$m and $l = 3x10^{-3}$m. As noticed, the ring thickness does not substantially affect the amplitude of the peaks and dips in R_L^{TM} but their frequency location. The deviations become larger as $k_0 L$ augments. Unless one has the problem of requiring special attenuation at a given particular frequency, Figure 3 shows that the R_L^{TM} is quite robust to variations in the ring thickness.

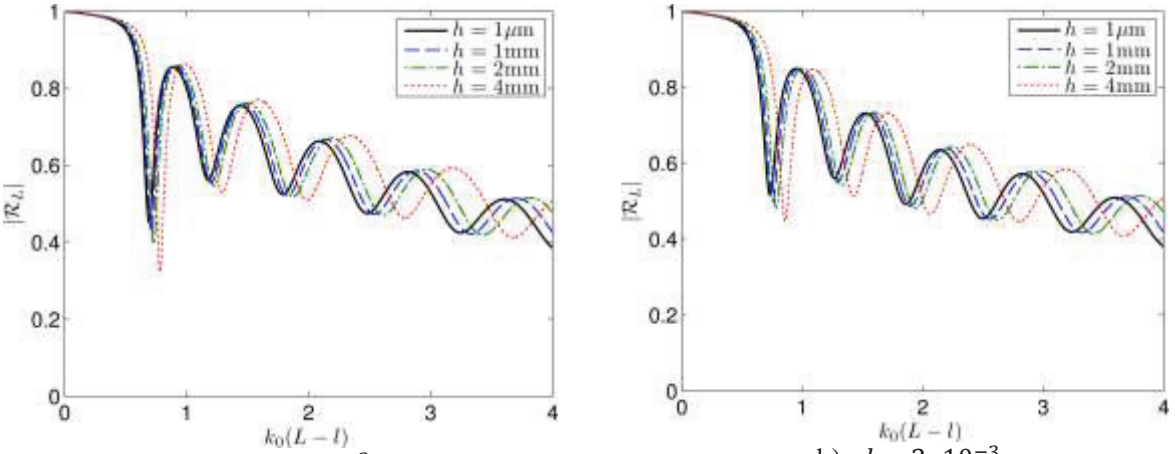

a) $l = 10^{-3}$m b) $l = 3x10^{-3}$m

Figure 5 – Influence of the ring thickness on the retarding structure reflection coefficient for fixed number of rings/cavities and damping.

4.4 Influence of damping

To conclude we will consider the effects of damping on R_L^{TM}. To that purpose, we will fix again the number of rings to $N = 40$ and the ring thickness to $h_r = 1\,\mu$m. As in the previous sections, we will also present results for the two imperfect ABHs with $l = 10^{-3}$m and $l = 3x10^{-3}$m. The damping has been modified by using the following values for the complex speed of sound $c = c_0(1 + \mu j)$, with $\mu = 0.01, 0.05, 0.1, 0.5$. The last values are unrealistic but have been included for illustrative purposes.

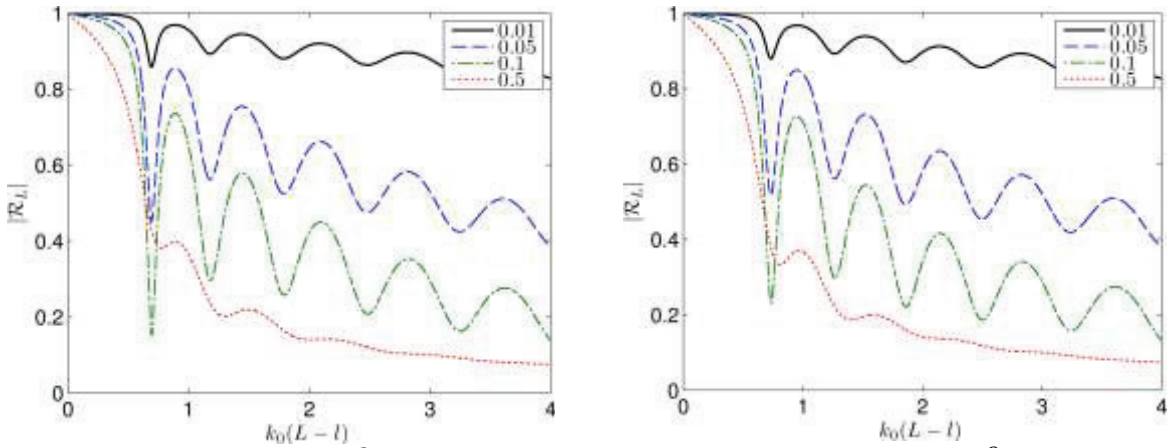

a) $l = 10^{-3}$m b) $l = 3x10^{-3}$m

Figure 6 – Influence of damping on the retarding structure reflection coefficient for fixed number of rings/cavities and ring thickness.

As one may have suspected, Figures 6a and b show that the damping plays a crucial role in the performance of the ABH. In practice yet, it turns out to be difficult to increase the retarding structure damping to lower its reflection coefficient. In [10,11], several attempts were made in that line, testing various configurations with absorbent material. However, the results were rather frustrating because the improvement of the ABH performance was not as expected. The authors of those works claimed an explanation is still missing for that behavior.

5. CONCLUSIONS

In this paper, we have suggested to analyze the ABH effect of retarding structures in duct terminations by means of the transfer matrix method. This allows one to make quick tests to determine the influence of the various parameters playing a role in practical realizations of the ABH. In particular, it has been observed that a huge number of rings/cavities are necessary to recover the reflection coefficient predicted by the theory. Besides, the ABH effect is quite robust to the variation of the ring thickness. The latter does not significantly alter the amplitude of the peaks and dips of the reflection coefficient but its frequency location. Finally and as expected, damping turns to be crucial to achieve low values of the reflection coefficient.

The reported analysis provides first indications on what to consider when building an ABH retarding structure. Yet, further issues are currently being investigated. For instance, it is barely justifiable that transfer matrices accounting for lateral cavities may correctly characterize the behavior of the initial rings at the entrance of the waveguide. Expansion chamber theory may prove better for that purpose. Finite element simulations will allow us to determine under which circumstances each approach becomes more adequate. Another topic being addressed is that of considering non-equispaced rings. Moreover, the results presented in this paper are being extended to quadratic acoustic black holes.

REFERENCES

1. Krylov VV. Acoustic black holes: recent developments in the theory and applications. IEEE Trans Ultrason Ferroelectr Freq Control. 2014; 61(8):1296:1306.
2. Krylov VV. New type of vibration dampers utilising the effect of acoustic ‘black holes’. Acta Acust united Ac. 2004; 90(5):830-837.
3. Krylov VV, Winward RETB. Experimental investigation of the acoustic black hole effect for flexural waves in tapered plates. J. Sound Vib. 2007; 300(1–2):43:49.
4. Georgiev VB, Cuenca J, Gautier F, Simon L, Krylov VV. Damping of structural vibrations in beams and elliptical plates using the acoustic black hole effect, J. Sound Vib. 2011;330 (11):2497:2508.
5. Denis V, Gautier F, Pelat A, Poittevin J. Measurement and modelling of the reflection coefficient of an acoustic black hole termination. J. Sound Vib. 2015; 349:67-79.
6. Conlon S, Fahnline J, Semperlotti F, Numerical analysis of the vibroacoustic properties of plates with embedded grids of acoustic black holes. J. Acoust. Soc. Am. 2015; 137(1):447:457.

7. Mironov MA, Pislyakov VV. One-dimensional acoustic waves in retarding structures with propagation velocity tending to zero. Acoust Phys. 2002; 48(3):347:352.
8. Climente A, Torrent D, Sánchez-Dehesa J. Omnidirectional broadband acoustic absorber based on metamaterials. Appl Phys Lett. 2012; 100(14):144103.
9. Elliott AS, Venegas R, Groby JP, Umnova O. Omnidirectional acoustic absorber with a porous core and a metamaterial matching layer. J Appl. Phys. 2014;115(20):204902.
10. El-Ouahabi AA, Krylov VV, O'Boy DJ. Experimental investigation of the acoustic black hole for sound absorption in air. Proc. ICSV22; 12-16 July 2015; Florence, Italy 2015.
11. El-Ouahabi AA, Krylov VV, O'Boy DJ. Investigation of the acoustic black hole termination for sound waves propagating in cylindrical waveguides. Proc. INTER-NOISE 2015; 9-12 August 2015; San Francisco, USA 2015.
12. Munjal ML. Acoustics of ducts and mufflers. Ed. John Wiley & Sons; 1987.